Mechanism of the Reaction $O^{16}+p \rightarrow p+4\alpha$ at 29 Mev*

OSCAR C. KOLAR

Lawrence Radiation Laboratory, University of California, Berkeley, California

(Received October 26, 1960)

An expansion cloud chamber containing oxygen gas at $\frac{1}{3}$ atmosphere pressure was used to study the reaction $O^{16}+p \rightarrow p+4\alpha$ at a bombarding energy of 28.9 Mev. Two hundred and twelve events were obtained that satisfied the criteria of energy and momentum balance. Ninety-one of these had all five outgoing prongs visible, while the remaining 121 had but four prongs visible, the fifth being obscured by the beam. Slightly more than half of all the events showed the presence of the ground state of Be^8. Of these, five events showed the presence of two Be^8 nuclei in the ground state. The events exhibiting the presence of a single ground-state Be^8 were interpreted according to the mechanism $O^{16}+p \rightarrow p+2\alpha+Be^8$; $Be^8 \rightarrow 2\alpha$. The possibility of a compound state was considered. If such an intermediate state did occur, it was such that it did not obey strictly the predictions of the compound-nucleus theory. The remaining half of the events did not show evidence for any intermediate nuclei (with the possible exception of the appearance of the 1.4-Mev state of B^9 in 5%, or fewer, of the cases) and could be interpreted only on the basis of the direct quadripartition of the oxygen nucleus.

I. INTRODUCTION

THE disintegration of oxygen into four alpha particles has been investigated intensively by many workers. Until now the reaction has been studied by using x rays to induce the reaction in nuclear emulsions.

The reaction was reported for the first time by Goward et al.,[1] using the Harwell AERE synchrotron, which produced a continuous x-ray spectrum that extended to 23 Mev. By 1950 these workers had obtained more than 100 such events.[2] On the basis of similar work done by Hänni et al.[3] on the photodisintegration of C^{12} into three alpha particles, the assumption was made that direct quadripartition was unlikely. On this basis, the mechanism was assumed to involve levels in Be^8 or C^{12}. Evidence was presented for the decay through a 9.7-Mev level in C^{12}, and thence through the ground state of Be^8 in 50 to 55% of the observed events. The remainder were assumed to proceed through undetermined levels of C^{12} and Be^8. The possibility of mechanisms involving the simultaneous emission of more than two particles was ignored.

By 1952 Goward and his co-workers had analyzed about 700 events.[4] These events were induced by 20- to 70-Mev x rays. The cross section as a function of energy revealed the presence of multiple resonances, suggesting that the process was to be interpreted in terms of excitation levels in a compound nucleus. By this time a few examples of the double production of Be^8 nuclei in the ground state had been observed.[5]

Livesy and Smith,[6] using x-ray energies extending to 32 Mev, presented evidence for the participation of C^{12} levels at 9.6, 11.3 ± 0.3, and 12.0 ± 0.3 Mev and another doubtful level at 16 Mev. According to these authors, these levels decayed through Be^8 levels at 3 and 4.3 ± 0.2 Mev as well as the ground state.

In 1953 Millar and Cameron[7] obtained 303 oxygen events, induced in emulsions by x rays. The maximum x-ray energy was 27 Mev. One hundred and nineteen of the events exhibited the presence of the ground state of Be^8. On the basis of the energy distribution of the alpha particles, however, it was observed that the participation of C^{12} levels was not consistent with the data obtained. These authors considered the possibility of more than two-body breakups and concluded that their results were to be explained by the mechanisms

$$O^{16}+\gamma \rightarrow 2\alpha+Be^8,$$

and

$$O^{16}+\gamma \rightarrow 4\alpha.$$

In the present experiment, it was proposed to extend the above results, using the proton beam of the Berkeley linear accelerator. For this purpose the cloud chamber was the ideal instrument, because a sufficiently low stopping power could be provided so that the resulting particles could escape from the beam. The event sought for was

$$O^{16}+p \rightarrow p+4\alpha.$$

This event can be readily distinguished from the other types of events appearing in the cloud chamber by the appearance of four heavily ionizing tracks along with a fifth lightly ionizing track emerging from the beam and coming from a common origin inside the beam. Frequently, one of the tracks is hidden by the proton beam, which traverses the cloud chamber in all the pictures. The total prong energy should be 14.5 Mev,

* This work was done under the auspices of the U. S. Atomic Energy Commission.

[1] F. K. Goward, E. W. Titterton, and J. J. Wilkins, Proc. Phys. Soc. (London) **A62**, 460 (1949).

[2] F. K. Goward and J. J. Wilkins, Proc. Phys. Soc. (London) **A63**, 1171 (1950).

[3] H. Hänni, V. L. Telegdi, and W. Zünti, Helv. Phys. Acta **21**, 203 (1948).

[4] F. K. Goward and J. J. Wilkins, Proc. Phys. Soc. (London) **A65**, 671 (1952).

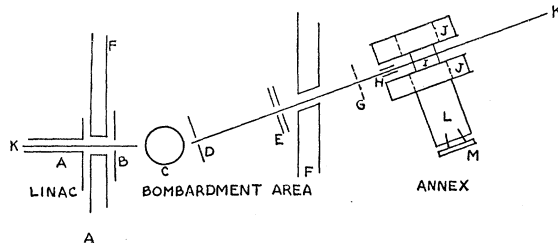[5] F. K. Goward and J. J. Wilkins, Proc. Phys. Soc. (London) **A64**, 94 (1951).

[6] D. L. Livesy and C. L. Smith, Proc. Phys. Soc. (London) **A66**, 689 (1953).

[7] C. H. Millar and A. G. W. Cameron, Can. J. Phys. **31**, 723 (1953).

FIG. 1. Plan view of the experimental geometry. A, high-energy end of linac. B, 4-jaw collimator. C, steering magnet. D, primary collimator. E, secondary collimator and clipper. F, walls of building. G, thin window at end of beam tube. H, ion chamber. I, cloud chamber. J, Helmholtz coils. K, proton beam. L, camera tube. M, stereoscopic camera.

corresponding to an incident proton energy of 28.9 Mev and a Q of 14.43 Mev.

In the following discussion, energy levels and Q values are cited frequently; unless otherwise specified the values used are those adopted in the review article by Ajzenberg and Lauritsen.[8]

II. EXPERIMENTAL TECHNIQUES

A. Proton Beam

The experimental apparatus consisted primarily of the cloud chamber with a pair of Helmholtz coils and the associated control equipment. These were located in the annex to the linear accelerator building. The setup is represented schematically in Fig. 1.

After a 10-deg deflection at the steering magnet, the beam passed through 25 ft of evacuated tubing, which was sealed at the exit end by a 0.001-in.-thick aluminum thin window. In the region where the stray field of the magnet was appreciable, the beam tube was of iron, which magnetically shielded the beam.

Upon emerging from the beam tube, the beam traversed a 6-in. air gap and entered the cloud chamber through another 0.001-in.-thick aluminum thin window. An air ionization chamber was situated in the air gap.

B. Cloud Chamber

The cylindrical, expansion-type cloud chamber was situated in the gap of a pair of Helmholtz coils, with its axis of revolution horizontal. The gas used was oxygen saturated with water vapor. The expanded pressure was $\frac{1}{3}$ atm. Further details, including photography and timing, are given elsewhere.[9]

The cloud chamber was provided with a pair of Helmholtz coils, which were energized by a 150-hp minesweeper generator with a 5-ton flywheel mounted between the motor and generator.[10] The peak field was 6870 gauss. The maximum rate of heat dissipation im-

posed a cycle time of 2 min, which was achieved by giving the cloud chamber two slow expansions followed by a 50-second waiting time. During these operations the ionization-chamber shutters were lowered, and the beam-intensity level was adjusted. The rise time of the current in the Helmholtz coils was 2.5 sec, and the current then remained constant at its peak value for about 0.2 sec.

III. ANALYSIS OF DATA

A. Reprojection

In order to measure the events, the pictures were reprojected in a projector which, except for a 45-deg front-surfaced mirror, duplicated the geometry of the original optical system. This projector has been described by Brueckner et al.[11] The pictures were projected on a translucent glass screen which could be oriented in any position to match the actual position of a track in space. By these means the space angles, radii of curvature, and ranges of the tracks could be accurately measured.

B. Initial Criteria

The film was scanned in the projector, each possible event being measured immediately. The initial requirements were that four or five prongs be perceptible, but that not more than one have an apparent ionization low enough to correspond to that of a proton, and that all the prongs intersect at the same point within the beam. For those events satisfying the above requirements all the tracks were lined up successively. If all the tracks aligned at the same height, the event was then said to satisfy the initial criteria and all its prongs were then carefully measured. This procedure led finally to the measurement of 300 possible events.

C. Data Recorded

The raw data were recorded directly on especially printed Keysort cards, with one track per card. For the event as a whole, the information recorded included the picture frame number, the distance S of the origin from the point of entry of the beam, the height of the origin, and the number of prongs visible. For individual tracks that went out of the illuminated region, the information recorded included the prong identity, the dip angle α, the beam angle β_M, the slant radius ρ_S, the distance D from the center of the track to the center of the chamber, the estimated relative ionization, and the error $\delta\rho_S$ to which the slant-radius measurement was subject. The slant radius ρ_S was measured in the plane of the track by means of transparent templates on which circular arcs of varying radii were scribed. The error $\delta\rho_S$ was obtained from a nomograph of the relation $\delta\rho_S = 0.08(\rho_S/L)^2$, which assumes an error of 0.1 mm in the sagitta in matching the template to the track. The

[8] F. Ajzenberg and T. Lauritsen, Revs. Modern Phys. **27**, 77 (1955).

[9] J. L. Need, University of California Radiation Laboratory Report UCRL-2806, December 3, 1954 (unpublished); Phys. Rev. **99**, 1356–66 (1955).

[10] W. M. Powell, Rev. Sci. Instr. **20**, 403 (1949).

[11] K. Brueckner, W. Hartsough, E. Hayward, and W. M. Powell, Phys. Rev. **75**, 555 (1949).

chord length of the track is L. For tracks that stopped in the illuminated region of the chamber, the data recorded were prong identity, dip angle α, beam angle β_M, and range R.

D. Beam Angle β_B and Beam Energy

In order to determine the beam angle for the beam itself, β_B as a function of S, the beam was attenuated so as to show the traversal of 20 to 100 protons for several pictures during each run. From these pictures it was possible to distinguish individual proton tracks.

Need had previously determined the beam energy to be 28.9 ± 0.5 Mev.[9] This value is used in this experiment. Need's determination was for the same geometry and represented an average over the same period of time as was involved in this experiment. A check for consistency was carried out by averaging the prong energies for the accepted events and adding the Q of the reaction. The result was 29.1 Mev, which is in good agreement with Need's value and may be considered to lend plausibility to the range-energy relation used.

E. Magnetic Field

The momentum of a particle producing a track in a cloud chamber is proportional to the product $B\rho s$, so that an accurate knowledge of the field of the Helmholtz coils was required. The field was measured by use of a search coil and integrator. The quoted accuracy of this measurement was $\pm0.3\%$.

The field was found to be nearly symmetric axially, so that the only variation included in the calculations was the radial variation. To this end a table was prepared that gives the magnetic field as a function of the ammeter reading and the radial distance D.
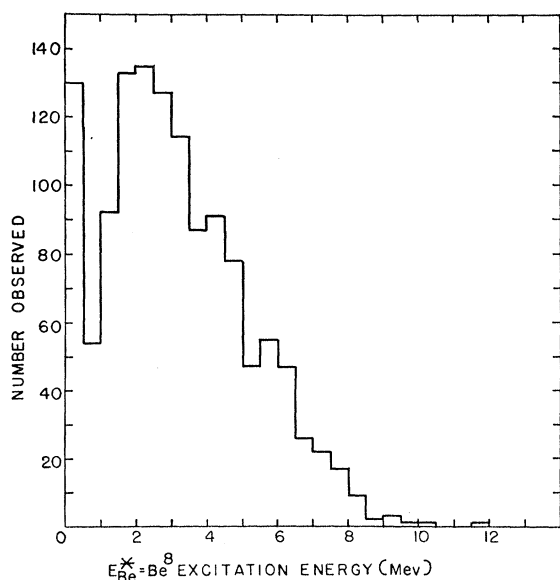
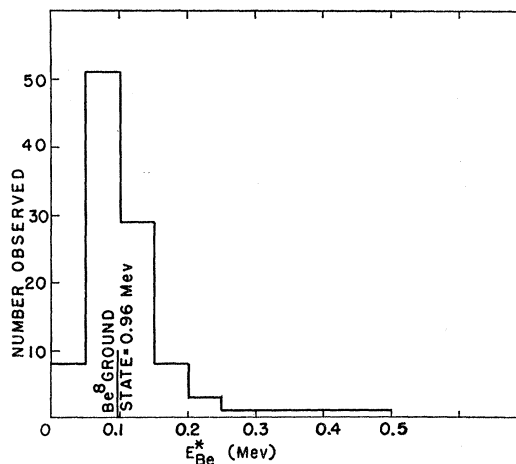

FIG. 2. Total distribution of Be^8 excitation energies.

FIG. 3. Distribution of E_{Be}^* values identified as Be^8 ground-state values.

F. Momentum-Energy Balance

The energy and rectangular components of momentum were calculated for each prong and were then summed for all prongs belonging to a given event that satisfied the initial criteria. Energy and momentum were required to balance within the calculated errors. Where only four prongs were visible, the energy balance only could be checked.

All events failing to achieve a satisfactory balance after the first measurement were independently remeasured and recalculated with the use of the average values obtained for the measured quantities. The same criteria for acceptance were adhered to. Finally all remaining events were measured for the third time by an independent observer. Events accepted on the basis of the third measurement usually were found to have been subject originally to faulty prong identification.

Of the 300 assumed events, 212 were finally accepted on the basis of the above requirements. Of the 88 rejected events, 68 were clearly of doubtful character, while the remaining 20 may have been events of the type of interest, but incapable of achieving balance for some unknown reason.

IV. RESULTS

A. Calculation of Be^8 Excitation Energy

During the measurement of the events it was noticed that many involved pairs of alpha particles with very small angular separation. This immediately suggested the possibility of the participation of the Be^8 ground-state nucleus in an intermediate stage of the reaction.

In order to verify this conjecture, it was necessary to calculate possible values of Be^8 excitation energy E_{Be}^*. There were four alpha particles in each event; consequently it was necessary to calculate six such E_{Be}^* values per event. Here E_{Be}^* is given by

$$E_{Be}^* = \tfrac{1}{2}(E_i+E_j) - (E_iE_j)^{\frac{1}{2}} \cos\phi_{ij},$$

where E_i and E_j are the kinetic energies of the two alpha particles and ϕ_{ij} is their angular separation. The distribution of $E_{Be}*$ values so obtained is presented in Fig. 2 in histogram form. In the interpretation of this diagram one should bear in mind that of the six $E_{Be}*$ values calculated for a given event, two at the very most can have physical significance. Consequently, if states of Be⁸ did participate, they would be expected to manifest themselves in the form of peaks superimposed on a continuous background of nonsignificant $E_{Be}*$ values.

The large peak in the interval 0 to 0.5 Mev certainly supports the observation that many events involved the Be⁸ ground state. Figure 3 presents an enlarged view of the $E_{Be}*$ distribution for the interval 0 to 0.5 Mev. This figure omits only the nine events that had more than one $E_{Be}*$ <0.5 Mev, and which arose from alpha pairs having an alpha particle in common. The unweighted

TABLE I. Summary of possible reaction mechanisms for the reaction $p+O^{16} \to p+4\alpha$. (The decays of Be⁸ and Li⁵ nuclei are not indicated.)

Initial step of reaction mechanism	Subsequent steps if a single Be⁸ ground-state nucleus may appear	Subsequent steps if no Be⁸ ground-state nucleus appears	Degree of participation in observed events	Mechanism number
$O^{16}+p \to F^{17*}$	any complete mechanism listed below	any complete mechanism listed below	results probably cannot be interpreted on basis of compound nucleus theory	(1)
$O^{16}+p \to Li^5+C^{12*}$	$C^{12*} \to \alpha+Be^8$		negligible	(2a)
		$C^{12*} \to \alpha+Be^{8*}$	negligible	(2b)
		$C^{12*} \to 3\alpha$	negligible	(2c)
$O^{16}+p \to Li^{5*}+C^{12*}$	$C^{12*} \to \alpha+Be^8$		<10% with (14)	(3a)
		$C^{12*} \to \alpha+Be^{8*}$	negligible	(3b)
		$C^{12*} \to 3\alpha$	negligible	(3c)
$O^{16}+p \to B^9+Be^8$	$B^9 \to p+Be^{8*}$		negligible	(4a)
	$B^9 \to p+2\alpha$		negligible	(4b)
$O^{16}+p \to B^{9*}+Be^8$	$B^{9*} \to p+Be^{8*}$		negligible	(5a)
	$B^{9*} \to p+2\alpha$		negligible	(5b)
$O^{16}+p \to B^9+Be^{8*}$	$B^9 \to p+Be^8$		negligible	(6a)
		$B^9 \to p+Be^{8*}$	negligible	(6b)
		$B^9 \to p+2\alpha$	negligible	(6c)
$O^{16}+p \to B^{9*}+Be^{8*}$	$B^{9*} \to p+Be^8$		negligible	(7a)
		$B^{9*} \to p+Be^{8*}$	} <5% with (12h), (12i), (19b), and (19c)	(7b)
		$B^{9*} \to p+2\alpha$		(7c)
$O^{16}+p \to p+O^{16*}$	(10), (17a), or (20)	(11), (17b), (17c), (21) or (24)	inconclusive	(8a)
			inconclusive	(8b)
$O^{16}+p \to p+2 Be^8$			see section B	(9)
$O^{16}+p \to p+Be^8+Be^{8*}$			negligible	(10)
$O^{16}+p \to p+2Be^{8*}$			negligible	(11)
$O^{16}+p \to \alpha+N^{13*}$	$N^{13*} \to p+C^{12*}$, $C^{12*} \to \alpha+Be^8$		negligible	(12a)
	$N^{13*} \to \alpha+B^9$, $B^9 \to p+Be^8$		negligible	(12b)
	$N^{13*} \to \alpha+B^{9*}$, $B^{9*} \to p+Be^8$		negligible	(12c)
$O^{16}+p \to \alpha+N^{13*}$		$N^{13*} \to p+C^{12*}$, $C^{12*} \to \alpha+Be^{8*}$	negligible	(12d)
		$N^{13*} \to p+C^{12*}$, $C^{12*} \to 3\alpha$	negligible	(12e)
		$N^{13*} \to \alpha+B^9$, $B^9 \to p+Be^{8*}$	negligible	(12f)
		$N^{13*} \to \alpha+B^9$, $B^9 \to p+2\alpha$	negligible	(12g)
		$N^{13*} \to \alpha+B^{9*}$, $B^{9*} \to p+Be^{8*}$	} <5% with (7b), (7c), (19b) and (19c)	(12h)
		$N^{13*} \to \alpha+B^{9*}$, $B^{9*} \to p+2\alpha$		(12i)
$O^{16}+p \to \alpha+Li^5+Be^8$			negligible	(13)
$O^{16}+p \to \alpha+Li^{5*}+Be^8$			<10% with (3a)	(14)
$O^{16}+p \to \alpha+Li^5+Be^{8*}$			negligible	(15)
$O^{16}+p \to \alpha+Li^{5*}+Be^{8*}$			negligible	(16)

TABLE I—*Continued.*

Initial step of reaction mechanism	Subsequent steps if a single Be^8 ground-state nucleus may appear	Subsequent steps if no Be^8 ground-state nucleus appears	Degree of participation in observed events	Mechanism number
$O^{16}+p \rightarrow p+\alpha+C^{12*}$	$C^{12*} \rightarrow \alpha+Be^8$		$<7\%$	(17a)
		$C^{12*} \rightarrow \alpha+Be^{8*}$	negligible	(17b)
		$C^{12*} \rightarrow 3\alpha$	negligible	(17c)
$O^{16}+p \rightarrow 2\alpha+B^9$	$B^9 \rightarrow p+Be^8$		negligible	(18a)
		$B^9 \rightarrow p+Be^{8*}$	negligible	(18b)
		$B^9 \rightarrow p+2\alpha$	negligible	(18c)
$O^{16}+p \rightarrow 2\alpha+B^{9*}$	$B^{9*} \rightarrow p+Be^8$		negligible	(19a)
		$B^{9*} \rightarrow p+Be^{8*}$	$\left.\rule{0pt}{12pt}\right\}<5\%$ with (7b), (7c),	(19b)
		$B^{9*} \rightarrow p+2\alpha$	(12h), and (12i)	(19c)
$O^{16}+p \rightarrow p+2\alpha+Be^8$			Probably accounts for majority of events involving a single Be^8 ground-state nucleus	(20)
$O^{16}+p \rightarrow p+2\alpha+Be^{8*}$			negligible	(21)
$O^{16}+p \rightarrow 3\alpha+Li^5$			negligible	(22)
$O^{16}+p \rightarrow 3\alpha+Li^{5*}$			negligible	(23)
$O^{16}+p \rightarrow p+4\alpha$			Probably accounts for majority of events involving no Be^8 ground-state nucleus	(24)

average of these E_{Be}^* values was 114 kev, which compares favorably with the accepted value of 96 kev (E_{Be}^* being measured relative to the state of two separate alpha particles).

The 94 events with a single E_{Be}^* value of <0.5 Mev were considered to involve the Be^8 ground state. So too, were five events that had two such E_{Be}^* values arising from pairs of alphas with no alpha common to the two pairs. In addition, the nine events with several such E_{Be}^* values were included in this category but were not used in subsequent calculations, since the identity of the alpha pair arising from the Be^8 ground state was not known.
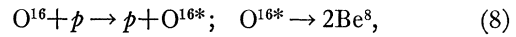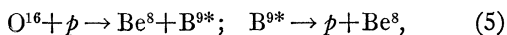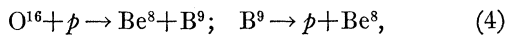
Figure 4 shows the appearance of an event interpreted as proceeding via the ground state of Be^8. The two alphas on the concave side of the beam are those attributed to the Be^8 ground-state decay.

The next state of Be^8 that could be expected to participate is the broad 3-Mev level. Figure 2 shows that this state cannot be present to a significant extent, since the distribution is decreasing smoothly through the value $E_{Be}^*=3$ Mev. The possibility of the participation of this state is considered again, below.

Table I lists all possible initial steps for the reaction mechanism and classifies the initial steps further as to the possibility for the participation of the Be^8 ground state. These mechanisms are considered in more detail in the following sections.

B. Events Exhibiting Two Be^8 Ground-State Nuclei

Reference to Table I shows that these five events could be accounted for by the following mechanisms:

$$O^{16}+p \rightarrow Be^8+B^9; \quad B^9 \rightarrow p+Be^8, \quad (4)$$

$$O^{16}+p \rightarrow Be^8+B^{9*}; \quad B^{9*} \rightarrow p+Be^8, \quad (5)$$

$$O^{16}+p \rightarrow p+O^{16*}; \quad O^{16*} \rightarrow 2Be^8, \quad (8)$$

$$O^{16}+p \rightarrow p+2Be^8. \quad (9)$$

If either mechanism (4) or (5) is the correct interpretation, kinematic limits on the proton energy could be calculated. None of the proton energies was found to be consistent with mechanism (4), but one event had a proton energy consistent with mechanism (5) if one assumed either the 1.4- or 2.37-Mev state of B^9.

The initial step of mechanism (8) is discussed in the following section. Evidence for or against the presence of an excited state of O^{16} may be considered as inconclusive for the reasons mentioned below; consequently, while it would appear reasonable that neither possibility (4) nor (5) may be considered as the dominant decay mode here, it is not possible to make a choice between mechanisms (8) and (9).

C. Events Exhibiting One Be^8 Ground-State Nucleus

Table I lists all the mechanisms that could involve a single Be^8 ground-state nucleus. The various possibilities are considered individually below.

Mechanism 1

This mechanism corresponds to the usual compound-nucleus interpretation of nuclear reactions. For low mass numbers this theory is generally held to be inapplicable. To check the degree of validity it is, however, desirable to make a few simple calculations. If the Coulomb barrier can be neglected, it is easy to show that if the protons are divided among energy intervals of constant size, a plot on semilog coordinate paper of the ratio of the number of protons falling in a given interval to the energy about which the interval is centered should yield a straight line. Since the protons
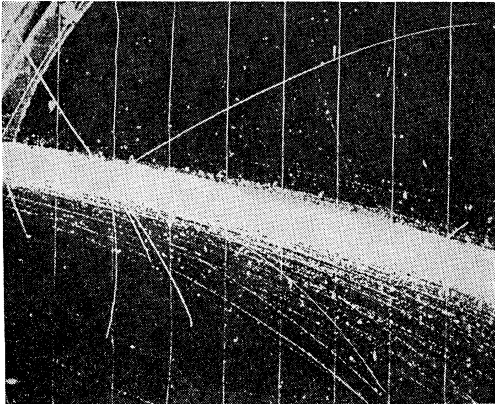
FIG. 4. An event involving the Be⁸ ground state. Two alpha particles on concave side of beam attributed to Be⁸ ground state.

are charged, however, a modification due to the Coulomb barrier should be expected. Figure 5 presents the distribution obtained for all events (since this step would be independent of the appearance of Be⁸), and it is seen that within the statistics a satisfactory fit is obtained with a straight line. The Coulomb barrier for oxygen has the value 3.2 Mev, and the relatively large number of protons (about 50%) with energies less than this value would certainly seem to indicate that the predictions of the compound-nucleus theory are not valid for this reaction. Similar results have been obtained by other workers.[12,13]

A further check is provided by the calculation of the forward-to-backward ratio of the number of protons in
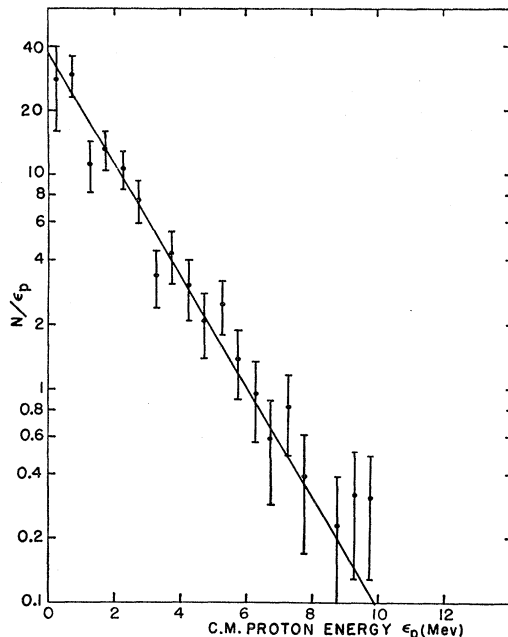
FIG. 5. N/ϵ_p for protons from all events vs proton energy (c.m.), ϵ_p.

[12] E. G. Silver and R. W. Waniek, Phys. Rev. **95**, 586 (1954).
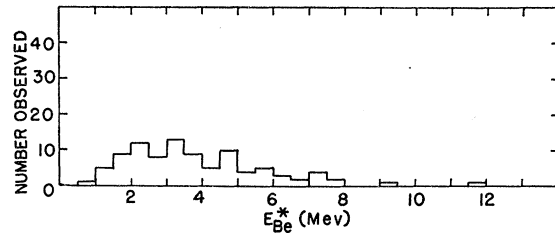[13] J. Benveniste (private communication).

FIG. 6. $E_{Be}*$ distribution for alpha pairs opposite to those identified as arising from Be⁸ ground-state decay.

the center-of-mass system. According to theory, this ratio should have the value unity. In this experiment, if the ratio is taken for all protons independently of their energy, the ratio is found to be 1.5 ± 0.2, which is, again, in disagreement with the compound-nucleus theory.

The above arguments are not intended to refute the participation of a compound state, but merely show that the usual compound-nucleus theory does not apply satisfactorily to these results. Thus, any or all of the initial steps of the mechanism in Table I may be considered to be preceded by the formation of a compound state, where the compound state does not strictly obey the predictions of the compound-nucleus theory. The following results are independent of the existence of such an intermediate state.

Mechanisms (2a) and (3a)

Kinematic limits on the proton center-of-mass energy were calculated. Virtually all events were found to exhibit proton energies consistent with these limits, and these results could only be considered as inconclusive. Possible excitation energies of the Li⁵ nuclei and C¹² nuclei could still be calculated. This was done, and is discussed below in connection with mechanisms (13), (14), and (17a).

Mechanisms (4a), (5a), (6a), (7a), and (10)

All these mechanisms are characterized by the appearance of an excited Be⁸ nucleus in addition to the ground-state Be⁸. If any of these mechanisms is a dominant mode, it should reveal itself in a plot of the $E_{Be}*$ values for the alpha pairs opposite to the pair originating from the ground-state Be⁸. This plot, then, should represent the level structure of Be⁸ with no obscuring continuum. Figure 6 presents the distribution obtained, and from the absence of peaks at the expected positions it is evident that none of these mechanisms can contribute to an appreciable extent.

Mechanisms (4b) and (5b)

The initial steps of these possibilities are two-body processes, and the center-of-mass kinetic energy of the Be⁸ nucleus should have one of several unique values. Assuming a 0.4-Mev uncertainty in the Be⁸ kinetic energies ϵ_{Be}, we found only four events to be consistent

with the B^9 ground state or the levels at 1.4 and 2.37 Mev. If we assume that higher levels of B^9 may participate, then peaks in the ϵ_{Be} distribution should be observed. Such was not the case, and it is clear that these possibilities may be rejected. These same considerations apply equally well to mechanisms (4a) and (5a) and are presented as additional evidence for their rejection.

Mechanism (8a)

For this mechanism the distribution of proton center-of-mass kinetic energy should exhibit peaks unless the O^{16} excitation energy is in a region where the level separation is small compared to the energy resolution available. (The average relative uncertainty in the proton energy was 26%; the average absolute uncertainty 0.9 Mev.) Should the latter be the case, this experiment would be inadequate to demonstrate the participation of this mechanism. The distribution obtained is presented in Fig. 7. It is apparent that if proton groups are present they are not revealed by this experiment. Because of the limitations due to energy resolution and statistics, this result is inconclusive.

Mechanism (12a)

Proton-emitting levels in N^{13} have been observed at 6.9 and 7.4 Mev. These levels, however, do not lie sufficiently high to allow for the subsequent breakup into three alphas of the resulting C^{12} nucleus.

If any higher levels of N^{13} contributed they would be expected to betray their presence in the form of peaks in the center-of-mass energy distribution of the two alpha particles not originating from the Be^8 ground-state nucleus. The peaks, if present, would be due to the first emitted alpha, and would be superimposed on a more or less continuous background due to the second alpha. From the distribution obtained (see Fig. 10), it is apparent that there is no significant indication of the presence of alpha groups. Further evidence for the nonparticipation of this mechanism will be presented in the discussion of mechanism (17a).

Mechanisms (12b) and (12c)

Again the energy distribution of the first two alpha particles should be expected to present peaks. As seen above, it does not. It is also possible to calculate the possible B^9 excitation energies. Since the B^9 nucleus
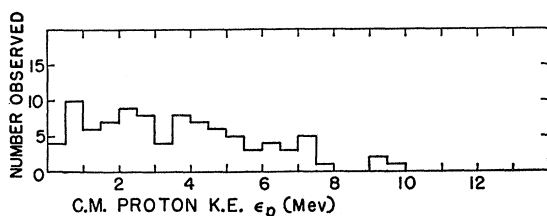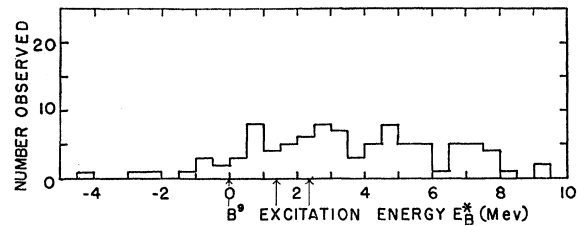

FIG. 8. Distribution of B^9 excitation energies E_B^* for Be^8 ground-state events.

must decay to the ground state of Be^8, the possible B^9 excitation energies E_B^* may be calculated uniquely for each event, and should either of these mechanisms be a dominant mode, the distribution of E_B^* values so obtained should represent the level structure of B^9 with no obscuring continuum. The distribution obtained is presented in Fig. 8, and there is no indication of the presence of B^9. The position of known levels of B^9 is indicated in Fig. 8 by the arrows on the axis of abscissas. The conclusion of the nonparticipation of B^9 states as indicated by the E_B^* distribution holds equally well for mechanisms (6a), (7a), (18a), and (19a), and is presented as additional evidence for their rejection.

Mechanisms (13) and (14)

The most satisfactory approach in these cases seemed to be the calculation of possible Li^5 excitation energies E_{Li}^*. Since the identity of the first alpha is not known, it was necessary to calculate two E_{Li}^* values per event, where one at most is significant. The E_{Li}^* values used measure the excitation of the Li^5 nucleus from the state of a separate proton and alpha, so that the ground and 2.5-Mev states, if present, will appear as peaks at $E_{Li}^*=1.8$ or 4.3 Mev. The distribution obtained is shown in Fig. 9. There is no statistically convincing evidence for the participation of Li^5 states, and we may set an upper limit of approximately 10% on the extent to which the 2.5-Mev state contributes, either through mechanism (3a) or mechanism (14).

Mechanisms (18a) and (19a)

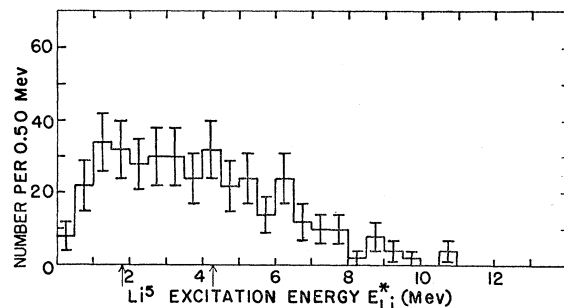Evidence concerning the possible participation of these mechanisms has already been presented in con-

FIG. 7. Distribution of energies (c.m.) for protons in Be^8 ground-state events.

FIG. 9. Distribution of Li^5 excitation energies E_{Li}^* for Be^8 ground-state events.

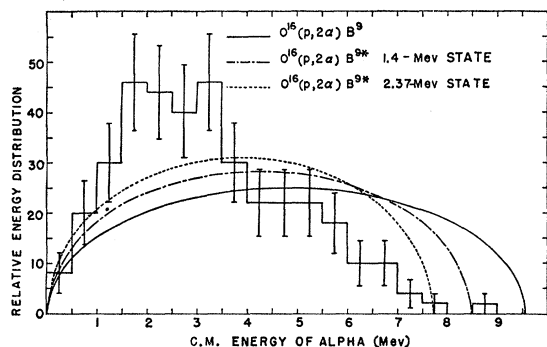FIG. 10. Distributions of energies (c.m.) of first two alphas for Be[8] ground-state events; comparison with distribution predicted for B[9] participation.

nection with mechanisms (12b) and (12c). The results of the E_B^* calculation described there would appear to rule out the participation of these mechanisms. An additional argument against mechanisms (18a) and (19a) is obtained by a comparison of the observed center-of-mass energy distribution of the first two alphas with that predicted on the basis of available phase space. On this basis the center-of-mass energy distribution of the first two alphas is given by[14]

$$f(\epsilon)d\epsilon = N\epsilon^{\frac{1}{2}}(E_m - \epsilon)^{\frac{1}{2}}d\epsilon,$$

where ϵ is the center-of-mass energy of the alpha, E_m is the maximum energy available to a single alpha, and N is a normalizing factor. Figure 10 is a plot of the distribution function computed for the ground state of B[9] as well as for the excited states at 1.4 and 2.37 Mev. The observed distribution is plotted in the same figure. It is apparent that the observed distribution cannot be accounted for very well on the basis of either of these proposed mechanisms.

Mechanism (17a)

Again, it is possible to construct an energy distribution function for the first two alpha particles. In this case the distribution function is not as simple as that obtained for mechanisms (18a) and (19a), because the second alpha is emitted from a moving C[12] nucleus. The calculated energy distribution for the 9.61-Mev level of C[12] is presented in Fig. 11 and compared with the observed distribution. The perturbations due to the Coulomb and angular-momentum barriers have not been included. These tend to decrease the numbers of low-energy and high-energy alphas. If these considerations are taken into account, it is seen that the agreement is satisfactory. However, this cannot be taken as conclusive evidence that this mechanism is the correct interpretation, because, as will be seen, mechanism (20) presents just as good agreement.

Consequently, it is again necessary to calculate

[14] G. E. Uhlenbeck and S. Goudsmit, *Pieter Zeeman 1865–1935* (Martinus Nijhoff, 'S Gravenhage, Netherlands, 1935), p. 201–211.
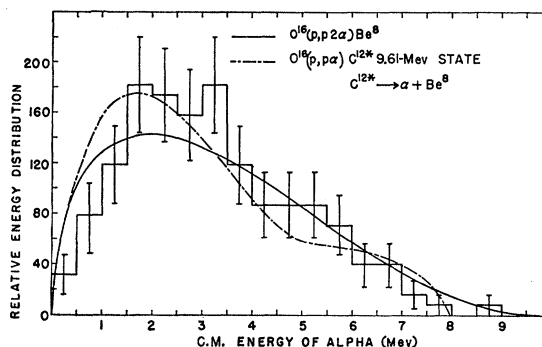

FIG. 11. Distributions of energies (c.m.) of first two alphas for events involving Be[8].

possible excitation energies E_C^* for intermediate C[12] nuclei. Two such E_C^* values must be calculated for each event. These results are given in Fig. 12, where the positions of peaks to be expected are indicated by the small arrows on the axis of abscissas. In addition to the levels indicated, alpha-emitting levels at 16, 20, and 25 Mev have been reported.[10] It is apparent that none of the latter levels appear, while the lower levels cannot be held to contribute to an appreciable extent. An upper limit of about 7% is set on the extent to which this mechanism contributes to the observed results.

Mechanism (20)

The center-of-mass energy distribution function in this case takes the form

$$f(\epsilon)d\epsilon = N\epsilon^{\frac{1}{2}}(E_m - \epsilon)^2 d\epsilon,$$

where the symbols have the same significance as they had in the distribution function appropriate to mechanisms (18a) and (19a). This function is shown in Fig. 11 along with the observed distribution. Recalling the effects to be expected from the perturbations due to Coulomb and angular-momentum barriers, we see that the agreement is quite good.

All other mechanisms disagree with the experimental results in one or more aspects, and the only conclusion is that this mechanism must be the correct interpretation for the majority of the events observed. It is interesting to note that this result is analogous to that obtained by Millar and Cameron[7] in their work on the photodisintegration of O[16].
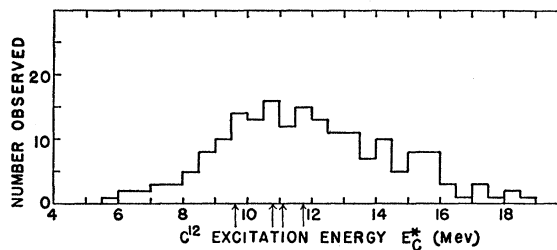
The results of this section are summarized in Table I.

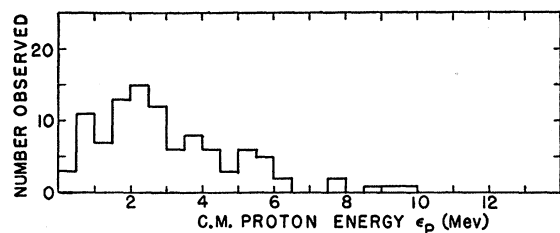FIG. 12. Distribution of C[12] excitation energies E_C^* for events involving Be[8] ground state.

FIG. 13. Distribution of energies (c.m.) for protons from events not exhibiting Be^8 ground states.

D. Events Exhibiting No Ground-State Be^8 Nuclei

Table I lists all possible reactions not proceeding through a ground-state Be^8 nucleus. The analysis of the 104 such events obtained is more complicated than that of the preceding events, since no clue is furnished to facilitate the calculations. For the most part it was found necessary to resort to possible excitation energies, as was done for some of the preceding possibilities. All mechanisms listed in Table I except Nos. (1), (8), and (24) must exhibit one or more excitation energies appropriate to levels in Li^5, Be^8, B^9, or C^{12}.

Mechanism (1)

This mechanism has already been discussed in connection with the events involving a single ground-state Be^8 nucleus and will not be considered further.

Mechanism (8b)

Again, a plot of the center-of-mass energies of the protons should result in peaks in the distribution, if this mechanism pertains and if this experiment is capable of resolving the levels.

Figure 13 shows the center-of-mass energy spectrum for the protons originating in events not involving the Be^8 ground state. The distribution obtained for this group is strikingly similar to that applying to the Be^8 ground state, and the same remarks must apply.

Mechanisms Involving Be^8 States

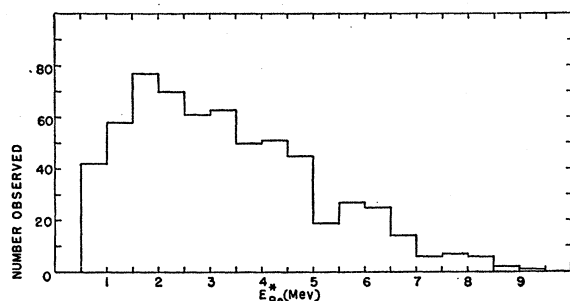Figure 14 presents the distribution of possible excitation energies $E_{Be}*$ for these events. Six such $E_{Be}*$

FIG. 14. Distribution of excitation energies $E_{Be}*$ for events not involving Be^8 ground state.

values are plotted for each event, and two at most can have physical significance. The first excited level of Be^8 lies at 2.90 Mev above the ground state. Since the excitation $E_{Be}*$ is measured from the state of two alphas, this level, if present, would be expected to appear in the form of a peak in the $E_{Be}*$ distribution, centered at 3.0 Mev. There is no evidence for the appearance of this level, nor are there any statistically significant peaks in the distribution that would indicate the participation of any higher levels. On this basis, all the possible mechanisms involving excited states of Be^8 may be rejected. All of these except (11) involve excited states of other nuclei, however, so that additional evidence in support of this conclusion will be presented in the form of other possible excitation-energy calculations.

Mechanisms Involving C^{12} States

Mechanisms (2c), (3c), (12e), and (17c) all involve the direct tripartition of an excited state of C^{12}. The disintegration of C^{12} into three alphas has been investigated intensively and, although it was sought for, no evidence for this mode of decay has been detected.[3,6,15-17] Accordingly, these mechanisms will not be considered further.

Four possible C^{12} excitation energies were calculated for each event, and Fig. 15 shows the distribution obtained. Of the four values plotted for each event, one, at most, can have physical meaning. If C^{12} states participate, they must appear as peaks at 9.61, 10.8, 11.1, and 11.74 Mev, and also possibly at higher levels. A peak centered at 11.75 Mev does appear, but its validity is dubious in light of the other similar peaks at spurious excitation energies. Furthermore, any states of C^{12} are constrained to decay through an excited state of Be^8 and, as we have seen, these do not appear. Consequently it would seem quite certain that C^{12} states do not participate to a greater extent than 10%, and it is probably safe to reject altogether such mechanisms involving excited states of C^{12}.
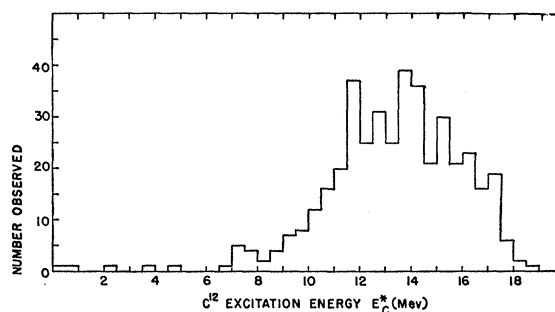

FIG. 15. Distribution of C^{12} excitation energy E_C* for all events not involving Be^8 ground state.

[15] L. L. Green and W. M. Gibson, Proc. Phys. Soc. (London) A62, 296 (1949).

[16] F. K. Goward, V. L. Telegdi, and J. J. Wilkins, Proc. Phys. Soc. (London) A63, 402 (1950).

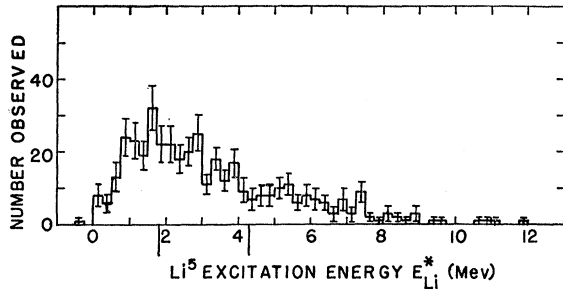[17] F. K. Goward and J. J. Wilkins, Proc. Phys. Soc. (London) A64, 93 (1951).

FIG. 16. Distribution of Li^5 excitation energies $E_{Li}*$ for events not exhibiting Be^8 ground state.

Mechanisms Involving Li^5 States

Four values of possible Li^5 excitation energies $E_{Li}*$ were calculated for each event. The distribution obtained is shown in Fig. 16. Again, peaks should appear at 1.8 and 4.3 Mev if Li^5 states participate. They do not.

Mechanisms Involving B^9 States

Six values of E_B* must be calculated for each event, and one at most can have physical significance. As before, E_B* denotes the possible excitation above the B^9 ground state. Figure 17 shows the observed distribution. The B^9 states, if present, should appear as peaks at 0, 1.4, and 2.37 Mev. In this case, there may be a small contribution from the 1.4-Mev state. An upper limit of 5% is set on the degree to which this state may participate. All that may be said regarding the small peak obtained is that it may be real, but could equally well be a statistical fluctuation.

Mechanism (24)

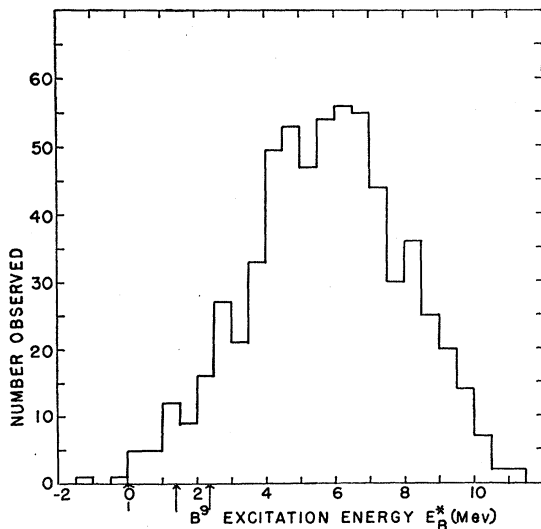This mechanism may be regarded as the direct quadripartition of O^{16} into four alpha particles. In this

FIG. 17. Distribution of B^9 excitation energies E_B* for events not involving Be^8 ground state.
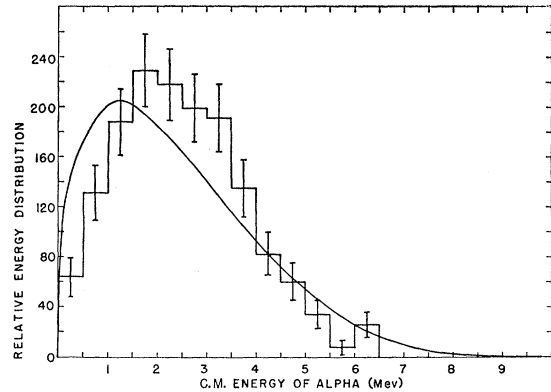

FIG. 18. Distribution of energies of all four alphas for events not involving Be^8 ground state. Energy-distribution function for quadripartition.

case we may again resort to statistical mechanics, and the form of the distribution function obtained for the four alphas is

$$f(\epsilon)d\epsilon = N\epsilon^{\frac{1}{2}}(E_\pi - \epsilon)^{7/2}d\epsilon,$$

where the symbols have the same significance as attributed to them above. Figure 18 gives this distribution function as well as the observed distribution. Bearing in mind the effects of the Coulomb and angular-momentum barriers, we see that the agreement is quite good. The similarity between Fig. 18 here and Fig. 30 of Millar and Cameron's article is striking. It seems quite certain that this mechanism does, indeed, represent the dominant mode for the 104 events not involving the Be^8 ground state.

Summary for Events Not Involving the Be^8 Ground State

No convincing evidence was found for the participation of Be^8 states, Li^5 states, or C^{12} states. The extent to which the 1.4-Mev state of B^9 may participate is limited to about 5%. All of the remainder would appear to decay by direct quadripartition. These results (except for the B^9 possibility) are again in agreement with those of Millar and Cameron.

ACKNOWLEDGMENTS

APPENDIXES

Appendix A. Errors

Maximum permissible errors were calculated for the resultant energy and momenta in each event by assuming the following errors in the angular measurements:

Angle (deg)	Error (deg)
$0 < \alpha < 60$	$\delta\alpha = \pm 1.5$
$\alpha = 60$	$\delta\alpha = \pm 2.0$
$\alpha > 60$	$\delta\alpha = \pm 2.5$
β_M	$\delta\beta_M = \pm 3$

Strictly speaking, these angular uncertainties are also functions of track length, but the above values were considered representative. These values are the same as those adopted by Brueckner et al.[11] except that $\delta\beta_M$ has been increased from 1 deg to 3 deg because of the presence of the beam. The above values were borne out well on remeasurement of the pictures.

The maximum error in particle energy due to uncertainty in the range-energy relation is a function of energy, but was ordinarily about 8%. The error in matching a scribed template to a curved track has been found to correspond to an error of 0.1 mm in the sagitta. Turbulence in the chamber was examined by use of weak-beam pictures without a magnetic field. The radius of curvature due to turbulence as determined by microscopic examination of single tracks was about 16 m. This was usually small compared to uncertainties due to other sources, and was omitted.

These errors were propagated and tables were constructed giving the resultant errors in energy and momentum components for individual tracks. The tables were accurate to about 5%. The resultant errors for an event were then taken to be the sums of the magnitudes of the individual errors, in order to facilitate the computations.

In the coordinate system used, the X and Y components of momentum should sum to zero, while the Z component should sum to the beam momentum. The standard deviations of the resultant momentum components for an individual event, as determined for all accepted events, were found to be:

$$\sigma P_X = 0.71 \times 10^5 \text{ gauss cm,}$$

$$\sigma P_Y = 0.52 \times 10^5 \text{ gauss cm,}$$

$$\sigma P_Z = 0.46 \times 10^5 \text{ gauss cm.}$$

The third value is to be compared with the value $(7.83 \pm 0.07) \times 10^5$ finally adopted for the beam momentum.

As previously mentioned, the weighted average of the beam-energy values for all accepted events was 29.1 Mev, and this value is to be compared with the accepted value 28.9 ± 0.5 Mev. The average obtained for all events with five prongs visible was 29.14 Mev, while that for all events with four prongs visible was 29.11 Mev.

Appendix B. Range-Energy Relation

Since nearly all the alpha particles stopped in the chamber, it was clearly desirable to establish the best range-energy relation possible. Fortunately, the stopping power of oxygen for protons has been published for the energy range 40 to 600 kev.[18] No experimental data beyond 600 kev are known to the author. Consequently, the use of theoretical values for the stopping power are required beyond this energy. Hirschfelder and Magee have published theoretical values of stopping power of oxygen for protons for the energy interval 0.005 to 3 Mev.[19] On comparison of these two sets of data, the experimental value was found to be appreciably larger than the theoretical value at low energies, but only 6% greater at 600 kev. To obtain values for energies up to 3 Mev, the experimental data were used up to 600 kev; beyond this energy the theoretical value adjusted to agree with the experimental value at 600 kev was used.

This was done by plotting the difference between the two sets of values as a function of energy and making a linear extrapolation to zero by matching the slope of this correction function at 600 kev. The correction to be applied to the theoretical values thus became zero at 1.1 Mev. This process, then, yielded the stopping power as a function of energy for 0.040- to 3-Mev protons.

The percentages of contaminants (as determined by the mass spectrometer) varied from run to run, and it was desirable to allow for their presence by use of a correction factor rather than by the actual construction for each run of curve of stopping power vs energy. This could be done because the stopping power of all the contaminants (except for the H_2 in the water vapor) was very near that of oxygen, and the percentages of contaminants were small. What was finally done was to assume the cloud chamber gas to be pure oxygen except for the H_2 in the water vapor. To check the reliability of this assumption, the range-energy relation was constructed by two methods for the run with the highest percentage of contaminants for the energy range of 40 to 600 kev. This was the range in which experimental values of stopping power were known. First, a stopping power-vs-energy curve was obtained by adding the stopping powers of the several components. This was then integrated numerically to give range as a function of energy. Second, the gas was assumed to be pure oxygen, allowing only for the presence of H_2 by means of a small correction. The percentage composition was 2.4% N_2, 0.6% A, 3.2% H_2O, and 93.8% O_2. The two ranges agreed to within 0.1 mm over the entire energy interval, and this was taken as justification of the above-mentioned assumption.

[18] H. K. Reynolds, D. N. F. Dunbar, W. A. Wenzel, and W. Whaling, Phys. Rev. **92**, 742 (1953).

[19] J. O. Hirschfelder and J. L. Magee, Phys. Rev. **73**, 207 (1948).

Tabulated values of water vapor pressure were used rather than the mass-spectrometer values, since these latter are not held to be reliable. The temperature of the cloud chamber was known immediately before expansion, so that the vapor pressure could be obtained from tables. This value of water vapor pressure was then

corrected to account for the known expansion ratio of the cloud chamber.

All that remained to be done at this point was to convert the proton ranges to alpha-particle ranges. The rule for this conversion is well-known for air and may be considered to be the same for oxygen.

Analysis of Some Deuteron-Induced Reactions in Oxygen-18†

J. C. Armstrong* and K. S. Quisenberry
Radiation Laboratory, University of Pittsburgh, Pittsburgh, Pennsylvania
(Received November 21, 1960)

The reactions $O^{18}(d,t)O^{17}$, $O^{18}(d,d')O^{18*}$, and $O^{18}(d,p)O^{19}$ are studied using 15-Mev deuterons and magnetic analysis of reaction particles. Absolute cross sections are determined for all reactions studied and the Butler-Born approximation is used to extract reduced widths when possible. Angular distributions of triton groups corresponding to the ground, 0.871-, 3.846-, 4.555-, 5.083-, and 5.378-Mev states of O^{17} are obtained. An estimate of the configuration admixtures in the O^{18} ground state is made from analysis of the reduced widths and indicates the presence of a sizable (about 6%) $(1f_{7/2}{}^2)_0$ component. The experimentally determined admixtures are compared with several theoretical estimates. All O^{18} levels observed in the inelastic deuteron scattering have been previously reported—the known 5.01-Mev state is not observed. The angular distribution of inelastic deuterons corresponding to the 1.982-Mev state of O^{18} is obtained and comparison of the absolute cross section with theory provides an estimate of the O^{18} deformation. Proton groups from $O^{18}(d,p)O^{19}$ reactions are observed corresponding to O^{19} excitations of 0, 1.469, 3.164, 3.948, (4.123), (4.586), (4.706), (5.165), 5.45, 5.707, and 6.279 Mev, where assignment of the levels in parentheses to O^{19} is uncertain. The known 0.096-Mev state is not observed and the proton group corresponding to 5.45-Mev excitation contains contributions from at least two states. Angular distributions leading to the O^{19} ground, 1.469-, 3.164-, 3.948-, 5.707-, and 6.279-Mev states are obtained and reduced widths extracted. The l_n values for these angular distributions are ambiguous except for the ground-state reaction $(l_n=2)$ and the 1.469-Mev state reaction $(l_n=0)$. Analysis of the data suggests that J^π (ground state)$=\frac{5}{2}^+$ and J^π (0.096-Mev state)$=\frac{3}{2}^+$. Using parameter values estimated from the O^{19} energy level spectrum or obtained from neighboring nuclei, a description of this nucleus in terms of the strong-coupling unified model agrees with the data.

I. INTRODUCTION

IN recent years nuclei just beyond O^{16}, at the beginning of the $1d$-$2s$ shell, have become increasingly important in the study of nuclear structure. They lie in a rather ill-defined region between nuclei described by shell model calculations $(A \leqslant 17)$ and others described by the Bohr-Mottleson strong-coupling unified model[1] $(A \approx 25)$. A theoretical description of the nuclei at the beginning of the $1d$-$2s$ shell may be possible solely in terms of one or the other of these two models, but will probably be complicated by interplay between independent-particle and collective effects.

Intermediate coupling calculations have been carried out for nuclei of $A = 18$ and 19 and satisfactorily explain the static properties of F^{18}, F^{19}, O^{18}, and O^{19}.[2-4] Such calculations provide strong evidence for the validity

of an individual-particle, intermediate-coupling approach to these nuclei even though weak surface-particle coupling must be added to account for observed $E2$ transition rates.[4,5] It is therefore surprising that F^{19} is also well described by the unified model in the strong-coupling limit.[6,7] Such a description implies the importance of collective effects in F^{19} and possibly in neighboring nuclei as well, and suggests that there exists a fundamental equivalence between the individual-particle and collective-model theories.[8]

A study of deuteron-induced reactions in O^{18} will provide information about several light $1d$-$2s$ nuclei and may serve to clarify certain theoretical aspects of their structure. Analysis of the (d,t) reaction data should provide information about O^{17} but, more important, it may be used to deduce configuration admixtures in the O^{18} ground state. Inelastic deuteron scattering data are somewhat less informative, although recent theoretical studies indicate that nuclear deformations may possibly be obtained from inelastic scattering angular distri-

† Work done in the Sarah Mellon Scaife Radiation Laboratory and assisted by the joint program of the Office of Naval Research and the U. S. Atomic Energy commission.

* Now at Physics Department, University of Maryland, College Park, Maryland.

[1] A. Bohr and B. R. Mottelson, Kgl. Danske Videnskab. Selskab, Mat.-fys. Medd. 27, No. 16 (1955).

[2] M. G. Redlich, Phys. Rev. 95, 448 (1954).

[3] M. G. Redlich, Phys. Rev. 99, 1427 (1955).

[4] J. P. Elliott and B. H. Flowers, Proc. Roy. Soc. (London) 229, 536 (1955).

[5] F. C. Barker, Phil. Mag. 1, 329 (1956).

[6] E. B. Paul, Phil Mag. 2, 311 (1957).

[7] G. Rakavy, Nuclear Phys. 4, 375 (1957).

[8] See for example: M. G. Redlich, Phys. Rev. 110, 468 (1958); J. P. Elliott, Proc. Roy. Soc. (London) A245, 128 (1958); A245, 562 (1958).
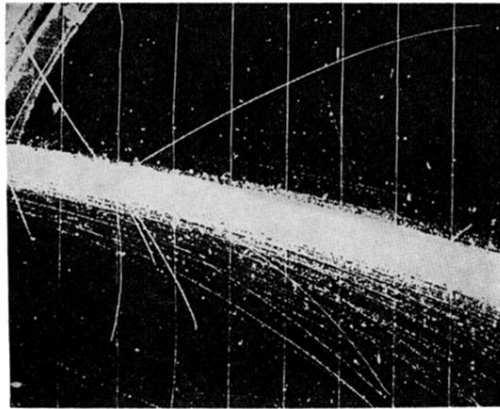
FIG. 4. An event involving the Be^8 ground state. Two alpha particles on concave side of beam attributed to Be^8 ground state.